Effects of Fluorine Substitution on the Structure and Dynamics of Complexes of Dihydrofolate Reductase (*Escherichia coli*)

E. Y. Lau and J. T. Gerig
Department of Chemistry, University of California, Santa Barbara, California 93106 USA

ABSTRACT Fluorine NMR experiments with a protein containing fluorinated amino acid analogs can often be used to probe structure and dynamics of the protein as well as conformational changes produced by binding of small molecules. The relevance of NMR experiments with fluorine-containing materials to characteristics of the corresponding native (nonfluorinated) proteins depends upon the extent to which these characteristics are altered by the presence of fluorine. The present work uses molecular dynamics simulations to explore the effects of replacement of tryptophan by 6-fluorotryptophan in folate and methotrexate complexes of the enzyme dihydrofolate reductase (DHFR) (*Escherichia coli*). Simulations of the folate-native enzyme complex produce local correlation times and order parameters that are generally in good agreement with experimental values. Simulations of the corresponding fluorotryptophan-containing system indicate that the structure and dynamics of this complex are scarcely changed by the presence of fluorinated amino acids. Calculations with the pharmacologically important methotrexate-enzyme complex predict dynamical behavior of the protein similar to that of the folate complex for both the fluorinated and native enzyme. It thus appears that, on the time scale sampled by these computer simulations, substitution of 6-fluorotryptophan for tryptophan has little effect on either the structures or dynamics of DHFR in these complexes.

INTRODUCTION

Biosynthetic incorporation of fluorinated amino acids into proteins has been demonstrated for over a dozen different analogs (Hortin and Boime, 1983). Classical synthetic methods and more recent in vitro enzymatic methods can provide peptides or proteins with a fluorinated residue at a single defined position (Wallace, 1978; Noren et al., 1989). Peptides and proteins containing fluorinated amino acids have utility in exploring or modifying the functional role of specific residues in biological activity. Moreover, proteins containing fluorinated amino acids can be examined profitably by fluorine NMR spectroscopy (Gerig, 1994) and, primarily because of the high sensitivity of the fluorine chemical shift parameter to local structure and environment, such experiments often provide useful information about conformational changes, protein association, or stoichiometry of binding interactions (Danielson and Falke, 1996).

From a chemical perspective, interactions between amino acid side chains are altered when a fluorinated amino acid replaces the corresponding native, nonfluorinated amino acid in a peptide or protein. Although the volume occupied by a covalent carbon-fluorine bond is similar to that occupied by the corresponding carbon-hydrogen bond (Gavezzotti, 1983; Nyberg and Faerman, 1985), the C-F bond is much more polar than a C-H bond (Smyth and McAlpine, 1934), so that new dipolar or electrostatic interactions are possible. Such interactions would include the formation of hydrogen bonds. Carbon-fluorine bonds are more hydrophobic or lipophilic than C-H bonds, and fluorine substitution could augment interactions between hydrophobic side chains (Leo et al., 1971). Finally, fluorine is more massive than hydrogen, so that the frequencies and amplitudes of molecular vibrations significantly involving the fluorine-substituted group will be changed relative to those of the corresponding native system. Potential consequences of any of these considerations is that fluorine substitution for hydrogen could alter the time-average positions of atoms in a protein as well as change the rates of conformational fluctuations. Experimentally, it is found that the presence of fluorinated amino acid analogs may alter the stability and biological activity of a protein or may have no effect (Gerig, 1994); a consistent picture of the effects of fluorine on protein structure or activity has not emerged.

Although placement of fluorinated amino acid analogs into proteins provides systems that are usefully studied by means of fluorine NMR experiments, it is not clear a priori that the conclusions reached through such observations are relevant to understanding the properties of the native system. It was the purpose of the present work to studied the effects of fluorine substitution on the structure and dynamics of a small protein by means of molecular dynamics (MD) simulations. Protein motions occur on a wide time scale (McCammon and Harvey, 1987), and such simulations are an effective way of exploring motions that take place in the time range 10^{-12} to 10^{-9} s. Such motions can be accessed experimentally by means of NMR relaxation studies (Wagner et al., 1993), and the characterization of rapid protein motions by such MD calculations are generally in accord with experimental observations (Smith and Dobson, 1996).

Received for publication 20 November 1996 and in final form 28 May 1997.

Address reprint requests to Dr. John T. Gerig, Department of Chemistry, University of California, Santa Barbara, CA 93106-0001. Tel: 805-893-2114; Fax: 805-893-4120; E-mail: gerig@nmr.ucsb.edu.

0006-3495/97/09/1579/14 $2.00

The enzyme dihydrofolate reductase (DHFR) from *Escherichia coli* was chosen for study in our work. This relatively small protein (159 residues) is present in all dividing cells, where it catalyzes the interconversion of 7,8-dihydrofolate and 5,6,7,8-tetrahydrofolate and aids in maintaining the necessary concentrations of folate coenzymes. DHFR has been well characterized mechanistically and structurally, such work being driven by its importance as a target for clinically significant antineoplastic and antibacterial drugs (Fierke et al., 1987; Penner and Frieden, 1987; Bystroff et al., 1990; Bystroff and Kraut, 1991; Blakley, 1995; Reyes et al., 1995). Experimental observations indicate that internal motions of the protein and of small molecules bound to the protein are important aspects of catalysis and inhibition of catalysis in this system (Searle et al., 1988; Farnum et al., 1991; Li et al., 1992). Dynamics of the DHFR backbone in the binary DHFR-folate complex have recently been characterized by means of ^{15}N NMR relaxation studies (Epstein et al., 1995).

Previous computational studies of DHFR have largely focused on the determination of free energy changes upon binding inhibitors or the NADPH cofactor (Singh, 1988; Singh and Benkovic, 1988; Cummins et al., 1991; McDonald and Brooks, 1992), although a study of domain motions in the *Lactobacillus casei* enzyme by dynamics sumulations has recently been reported (Verma et al., 1997). We show that computer simulations of molecular dynamics of the DHFR-folate complex and the structurally similar complex of DHFR with the drug methotrexate (MTX) are in accord with experimental observations. Computational studies of the corresponding DHFR-folate and DHFR-MTX complexes in which 6-fluorotryptophan replaces the tryptophan residues of the enzyme indicate that the fluorine substitutions in DHFR have only minor effects on the structures of these complexes or their dynamics over the time scale of 100 ps. Our calculations are thus consonant with the demonstration that the stability and activity of the 6-fluorotryptophan-substituted enzyme are nearly identical to those of the native enzyme (Hoeltzli and Frieden, 1994).

METHODS

All molecular dynamics simulations were performed according to the following general protocol, using CHARMM (Version 22.5; Brooks et al., 1983). All force-field parameters, except the partial atomic charges of the ligands, were obtained from the file PARM.PRM, which was included with the program QUANTA 3.2 (Molecular Simulations, Burlington, MA; Polygen, 1990). The 1–4 nonbonded interactions were scaled by one-half (Momany and Rone, 1992). Each simulation used all-atom representations of the protein, ligand, and solvent molecules. Except as detailed below, the initial heavy atom coordinates were those of crystal structures available from the Protein Data Bank (PDB).

The overall charge of a simulated system (DHFR, ligand, and solvent) was zero. For most simulations arginine, lysine, glutamate, and aspartate were modeled as neutral residues unless they were in the proximity of a charged group of a ligand. Folate and methotrexate were modeled as charged species; the overall charge of the system was neutralized by retaining charges on the side chains of Arg^{52} and Arg^{57}, which are near charges of the ligands.

Simulations of the fluorinated DHFR-MTX complex were performed with aspartate, glutamate, arginine, and lysine side chains with full charges. The net charge of DHFR-MTX in this case was −11 au. This system was neutralized by placing 11 Na^+ atoms in the proximity of carboxylate groups that were not involved in a salt bridge with either lysine or arginine. No constraints were placed on the enzyme, ligand, or counterions during these simulations.

For all simulations reported, the protein-ligand complex was surrounded by a collection of solvent water molecules. In forming the protein-solvent system, the complex was placed in the center of a droplet of water 35 Å in radius. The solvent sphere was sufficient in size that all protein atoms were at least 10 Å away from the solvent-vacuum interface. Any water molecule within 2.8 Å of any protein atom or a crystallographic water (if included in the simulation) was deleted. The TIP3P model for water was used in all simulations (Jorgensen et al., 1983). When crystallographic waters were included, all crystallographic waters in the PDB file were used and all were modeled as TIP3P waters. A typical simulation involved 16,762 atoms (protein, ligand, solvent) and included 4742 water molecules.

The SHAKE algorithm was not used in the simulations (Ryckaert et al., 1977). However, the TIP3P water was held rigid by increasing the angle bend force constant to 250 kcal mol^{-1} $radian^{-2}$. A harmonic constraint (k = 50 kcal mol^{-1} $Å^{-2}$) was placed on the oxygen atom of any water molecule more than 34 Å from the center of the sphere, to prevent "evaporation" of molecules from the droplet surface. As described further below, NOE constraints were placed on some structurally important water molecules.

After formation, the system was extensively potential energy minimized by a combination of steepest descents and Newton-Raphson methods before the molecular dynamics calculation was started. The system was then heated to 300 K in 5 ps and allowed to equilibrate for 20 ps, after which 100 ps of constant energy production dynamics was performed. The nonbonded potentials were cut off with smoothing functions to conserve the total energy of the system (Brooks et al., 1983). A switching function was used on the Lennard-Jones potential between 10 Å and 11 Å. The electrostatic potential was cut off by using a shifting function at 12 Å (Tasaki et al., 1993). The Verlet algorithm was used to integrate the equations of motion (Verlet, 1967). A time step of 1 fs was used for all simulations, and the nonbonded interactions were updated every 10 time steps. A dielectric constant of 1 was used in all simulations. All molecular dynamics runs were replicated, using different seed values for the random number generator.

Models of methotrexate and folate were built in QUANTA 4.0. The electrostatic charges for both molecules were assigned by the Gasteiger method as implemented in QUANTA (Gasteiger and Marsili, 1980). It should be noted that there can be some question of whether these charges are appropriate in the context of the CHARMM force field and these binary structures. However, the same approach apparently was used by Verma et al. (1997).

The crystal structures of the DHFR-folate complex (1DYI.ENT) and DHFR-methotrexate (4DFR.ENT) were used to provide starting coordinates (Bolin et al., 1982; Reyes et al., 1995). There are two crystallographic waters in the crystal structures of these complexes that have low Debye-Waller factors. These two water molecules appear to form extensive hydrogen bonds with the ligand and the protein; one of these has been postulated to be important in catalysis (Bystroff et al., 1990; Reyes et al., 1995). The two water molecules are located at corresponding positions in the crystal structures of DHFR from *L. casei* in a binary complex with MTX and DHFR from humans in a binary complex with folate (Bolin et al., 1982; Oefner et al., 1988). Nuclear Overhauser effects have been observed between these water molecules and the protein for the ternary complex of DHFR from *L. casei* (MTX and NADPH) and for the binary complex (MTX) and ternary complex (MTX and NADPH) from humans (Gerothanassis et al., 1992; Meiering et al., 1995; Meiering and Wagner, 1995). The NMR lifetimes of these water molecules in both the *L. casei* and human DHFR systems are in the nanosecond range, indicating that they are not transient entities, but part of a stable complex. Thus weak NOE constraints were placed on these two waters for our simulations. The force constant for all NOE constraints was 1 kcal mol^{-1} $Å^{-2}$. Eight such

constraints were used in the DHFR-folate simulations, whereas 11 constraints were present in the DHFR-methotrexate calculations. Omission of NOE constraints on the crystallographic waters from the calculations did not appear to have an appreciable effect on the backbone dynamics of the complexes.

For the fluorinated DHFR systems, all of the tryptophans in the DHFR portion of the models were replaced with 6-fluorotryptophan. The fluorinated amino acid was created by "mutating" the hydrogen attached at the 6 position of tryptophan to fluorine. The partial atomic charge used for fluorine was −0.25 au; the charge on the carbon bonded to the fluorine was adjusted to 0.25 au. These charges are consistent with ab initio calculations at the SCF/3–21G level for the 4-fluorophenyl group and with charges used in previous simulations of fluorinated amino acids and fluorobenzene (Gregory and Gerig, 1989, 1991; Pearson et al., 1993; Lau and Gerig, 1996).

Order parameters (S^2) were calculated for backbone N-H and C_α-H bonds as well as the $N_{\epsilon 1}$-$H_{\epsilon 1}$ bonds of the tryptophan residues. The autocorrelation function

$$C_2(t) = c\left\langle \frac{P_2[\mu(0) \cdot \mu(t)]}{r^3(0)r^3(t)} \right\rangle \quad (1)$$

was computed from snapshots of the dynamics trajectory taken at 0.1-ps intervals. Here $c = \langle r(t)^{-6} \rangle^{-1}$ serves as a normalization constant, μ is a normalized vector along the bond of interest, r is the bond length, and P_2 is the second-order Legendre polynomial. The normalization constant c ensures that the autocorrelation functions begin at 1 when $t = 0$. The order parameter S^2 was estimated by averaging the values of the autocorrelation function after it had decayed to a plateau (Palmer and Case, 1992). Typically, the data between 75 and 80 ps were used. In the case of glycine, the S^2 reported for the C_α-H bond vector is the average of the order parameters found for the two C_α-H bonds. The effective internal correlation time was calculated by using the following equation:

$$T_e = (1 - S^2)^{-1} \int_0^{80} [C_2(t) - S^2] dt \quad (2)$$

Debye-Waller (B) factors were calculated with Eq. 1, where Δr_i is the atomic displacement for atom i calculated from 100 ps of production dynamics, and the bracket indicates an average.

The rotation and diffusional motions were removed from the coordinate sets when the root mean squared deviation was calculated, by centering all of the protein atoms about the origin and then rotating the coordinates into alignment with the reference coordinate set. No attempt was made to remove possible effects of overall rotational diffusion of the protein when the correlation function was calculated, because it has been shown that these motions are on a different time scale and do not affect the correlation function or the subsequent S^2 and τ_e (Palmer and Case, 1992).

RESULTS

An eventual application intended for the work we carried out was examination of the role of dynamics in defining protein structure-induced fluorine chemical shifts. The only previous study of this nature used a computational model in which the ionizable amino acid side chains of the protein were treated as the corresponding neutral residues (Pearson et al., 1993). This approach was justified by the experimental observation that modification of surface charges of a protein by pH titration or acetylation of lysine side chains had little effect on fluorine chemical shifts of groups within the protein structure and the expectation that the charge of an ionized amino acid side chain at a protein is largely neutralized by nearby residues or ions of the medium that bear the opposite charge. We therefore considered two models of fluorotryptophan-containing DHFR. In one the side chains of Asp, Glu, His, Lys, and Arg are present in their neutral forms. For the second model these side chains were in the charge state that would be expected at neutral pH, with Asp and Glu negative, Lys and Arg positive, and His neutral. Sodium ions were included in these latter simulations to give an overall electrically neutral system.

Computational models of solvated native DHFR or DHFR with 6-fluorotryptophan residues in place of tryptophans were constructed from available crystallographic data and included ~5000 water molecules. The dynamics simulations used the facilities of the CHARMM package and the force field therein (Brooks et al., 1983). Typically, 100 ps of constant energy production dynamics was calculated after the system was heated to 300 K and equilibrated. Details of the models used and the simulations are given above.

Stability of the dynamics simulations

Stabilities of the computational models after temperature equilibration were examined in terms of the deviations of heavy atom positions from the positions found in the crystal structures that were used for construction of the computational model.

After extensive energy minimization, the root mean square deviation (RMSD) of the positions of heavy peptide backbone atoms of the DHFR-methotrexate complex compared to their positions in the crystal structure was 0.43 Å, when we used the model in which all side chains are electrically neutral. The same comparison for all heavy atoms of the protein-MTX complex led to a RMSD of 0.55 Å. Fig. 1 *a* presents a plot of the RMSD of the peptide backbone atoms as a function of simulation time in a dynamics simulation of the DHFR-MTX complex carried out as described above. The starting structure for the simulation was the energy-minimized model. After some initial drift, the RMSD of the heavy backbone atoms from the starting structure appears to fluctuate randomly in the range 0.93–1.3 Å. The RMSD of all atoms of the protein over the same time range was 1.4–1.9 Å. A duplicate simulation of this system, done with different initial velocities, behaved similarly, with the RMSD of the heavy backbone atoms found in the range 0.98–1.3 Å and the RMSD of all atoms ranging from 1.4 to 1.9 Å. The ranges of variation in backbone and all atom RMSDs observed in these and all of our simulations compare favorably with simulations by others of systems of similar complexity (Chandrasekhar et al., 1992; Philippopoulos and Lim, 1995).

A fluorine atom was introduced at the 6 position of each tryptophan residue in the initial DHFR-methotrexate model, and the energy of the system (with neutral side chains) was minimized. The RMSDs of the heavy atoms of this structure compared to the corresponding positions of atoms in the crystal structure of the native enzyme-MTX complex were

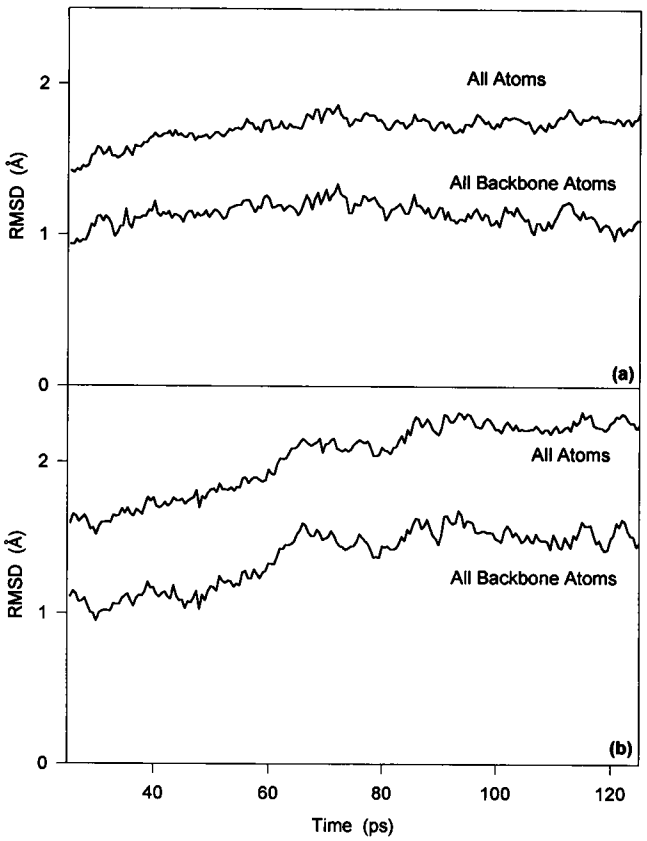

FIGURE 1 Root mean squared deviations of heavy atoms relative to their positions in the starting energy-minimized structure during molecular dynamics simulations. (*a*) Results for the native enzyme-MTX complex. (*b*) Results for the enzyme-MTX complex in which tryptophan residues of the protein have been replaced by 6-fluorotryptophan. In both cases all amino acid side chains were electrically neutral.

0.32 Å for the backbone atoms and 0.76 Å for all atoms. Comparing only heavy atoms within a 5-Å radius of a fluorine atom in the latter structure produced RMSD values between 0.4 and 0.9 Å, depending on the tryptophan residue examined. However, similar calculations comparing the positions of heavy atoms within 5 Å of the $C_{\eta 2}$ carbon atom of tryptophan residues in the nonfluorinated system to those found in the crystal structure indicated similar RMSDs from residue to residue. Thus the RMSDs from the crystal structure observed for heavy atoms in the vicinity of a 6-fluorotryptophan residue are not abnormal, and no effect on structure could be ascribed to the presence of fluorine. However, in both fluorinated and nonfluorinated DHFR-MTX complexes, deviations from the crystal structure of those heavy atom positions near Trp74 were appreciably larger than observed for the other tryptophan positions, at ~0.9 Å in both systems.

Fig. 1 *b* provides a plot of backbone RMSDs observed during a dynamics simulation of the DHFR-MTX complex in which all five tryptophan residues of the protein have been replaced by the 6-fluoro analog. As in the simulation of the native enzyme complex, some possible drift is apparent in the early phase of this simulation, but atom positions appear to fluctuate randomly about a mean later in the calculation. (The simulation represented in Fig. 1 *b* showed the largest initial drift of RMSDs of any simulation done for this work.) We found that simulations of systems containing fluorine generally exhibited slightly greater RMSDs of heavy atom positions than was observed in simulations of the corresponding native systems. For the simulation represented in Fig. 1 *b*, the RMSD for the heavy backbone atoms ranged from 0.95 to 1.6 Å, and for all atoms, from 1.6 to 2.3 Å. A duplicate simulation done with different initial velocities produced RMSDs for heavy backbone atoms of 0.82–1.2 Å and for all atoms of 1.3–1.7 Å. Considering the RMSDs for all simulations of the native DHFR-MTX complex and the form of this complex in which tryptophan has been replaced by 6-fluorotryptophan, there was no significant difference in the dynamics of heavy atoms.

The heavy atom RMSDs for DHFR-MTX in dynamics simulations of the model that has charged residues did not differ from those obtained from simulations using neutral side chains. One such simulation showed a range of 1.6–2.1 Å for all atoms and 1.1–1.4 Å for the heavy backbone atoms (Fig. 2 *a*); a replicate simulation had a slightly smaller RMSD range, 1.3–1.9 Å for all atoms and 0.88–1.5 Å for all heavy backbone atoms (Fig. 2 *b*). The ranges in the RMSDs

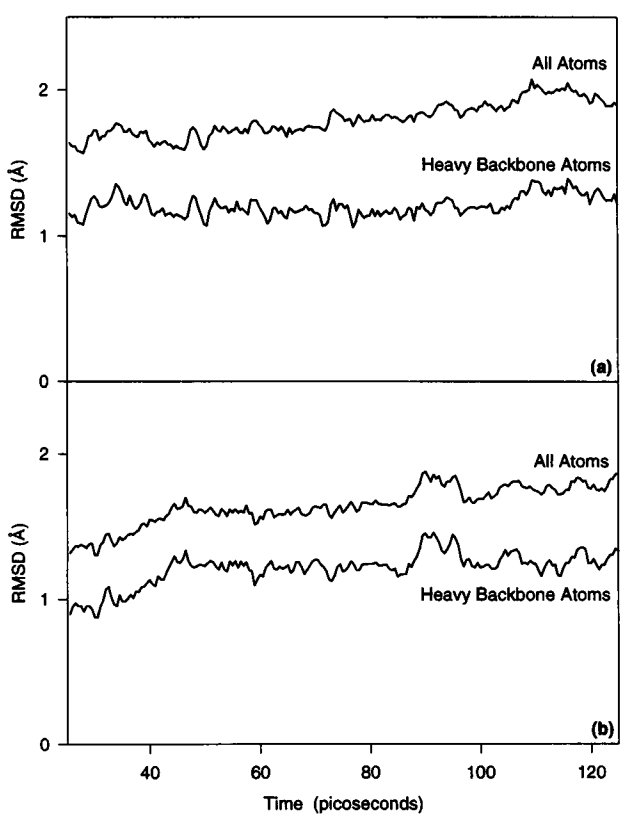

FIGURE 2 Root mean squared deviations of heavy atoms relative to their positions in the starting energy-minimized structure during MD simulations of 6-fluorotryptophan-containing DHFR-MTX complex using residues with fully charged Asp, Glu, Lys, and Arg side chain, as described under Methods. The simulations differ only in their initial velocities.

of the heavy atoms of DHFR in simulations using residues with full charges thus are similar to those obtained from simulations using neutral residues.

The binary complex between DHFR and its substrate folate were carried out in a similar manner. After energy minimization, the computational model of the native enzyme-folate complex had consistently smaller RMSDs of atom positions when compared to the corresponding crystal structure than were observed with DHFR-MTX complexes. The energy-minimized native DHFR-folate complex had a 0.29-Å RMSD for positions of the heavy backbone atoms relative to the corresponding crystal structure; the same comparison for all heavy atoms in the protein was 0.38 Å. Introduction of 6-fluorotryptophan into the DHFR-folate complex did not appear to significantly affect the protein structure. After energy minimization of the fluorinated DHFR-folate complex, the positions of the heavy backbone atoms had a 0.21-Å RMSD when compared to their positions in the crystal structure, whereas the RMSD for all heavy atoms after energy minimization was 0.26 Å. Again, the positions of atoms near a fluorine were not detectably affected in a specific way by the presence of the fluorine, showing RMSDs (0.19–0.29 Å) not appreciably different from the RMSDs of positions for atoms within 5 Å of the $C_{\eta 2}$ atom of a given tryptophan residue and typically 0.27–0.43 Å, depending on the residue. Interestingly, the RMSDs for atoms in the vicinity of Trp^{74} in the folate complex were 0.28 and 0.42 Å for the native and fluorinated complexes, respectively. The apparently high structural plasticity observed for this residue in the methotrexate complex is thus not apparent in the folate-enzyme complex.

Considering all of the simulations done, we observed essentially no difference in the RMSDs of heavy atoms during dynamics simulations of the native and fluorinated forms of the DHFR complexes. When comparing variations of atomic positions in simulations of native DHFR-ligand complexes and the corresponding fluorinated DHFR complexes, the differences between the fluorinated and nonfluorinated systems were no larger or more localized than the differences between replicate simulations of the native and fluorinated systems. It also appears that the charge state of Asp, Glu, His, Lys, and Arg side chains has little influence on dynamics of systems where 6-fluorotryptophan replaces the somewhat less polar tryptophan residues.

Isotropic B-factors

As a means of further accessing the dynamics simulations of the folate and MTX complexes of DHFR that were carried out, we calculated Debye-Waller factors. The Debye-Waller (B) factors produced during the analysis of diffraction data from protein crystals reflect thermal fluctuations of atomic positions, slower conformational changes such as aromatic ring rotation, and lattice disorder within the crystal (Petsko and Ringe, 1984). Presuming the absence of, or correction for, lattice disorder, a B-factor can be related to the mean square atomic fluctuation of an atom by Eq. 1 (McCammon and Harvey, 1987):

$$B_1 = \frac{8\pi^2\langle \Delta r_1^2 \rangle}{3} \tag{3}$$

In Fig. 3 *a* B-factors for the backbone amide nitrogens of DHFR in the enzyme-folate complex obtained from the crystal structure data of Reyes et al. (1995) are compared to B-factors calculated from one of our 100-ps dynamics simulations. The agreement between experiment and the computational results is good, primarily because the quality of the crystal structure is high (solved to a resolution of 1.9 Å, R = 13.7%), so that the contribution of lattice defects to the experimental B-factors is likely low. The correlation coefficient (r_c) for the B-factors from this simulation to the experimental B-factors is 0.43. The r_c for the replicate simulation is 0.34. The correlation coefficient found is approximately the same as has been found by comparisons of calculated B-factors with crystallographic data (Ichiye et al., 1986).

Fig. 3 *b* shows the amide nitrogen B-factors calculated from a dynamics simulation of the 6-fluorotryptophan-containing DHFR-folate complex. In this case there is a difference between the calculated B-factors for the fluorinated

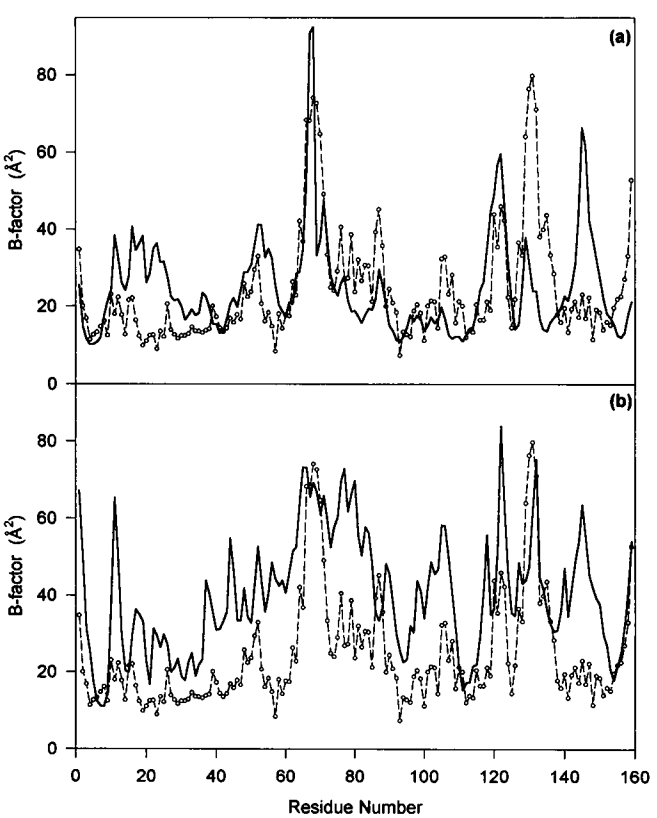

FIGURE 3 Comparison of calculated Debye-Waller B-factors (——) for backbone amide nitrogens with experiment (– – –). (*a*) Results from a simulation of the native DHFR-folate complex. (*b*) Results from a simulation of the enzyme-folate complex in which tryptophan residues of the protein have been replaced by 6-fluorotryptophan.

DHFR-folate complex relative to both experimental and calculated B-factors for the native structure, with the spatial fluctuations of the amide nitrogens in the fluorinated enzyme-folate complex being somewhat larger than those observed or calculated for the crystalline native DHFR-folate complex. Nonetheless, the general trends found for the native enzyme system are still fairly well reproduced by this simulation. Considering all simulations done, differences between calculated B-factors for the native and 6-fluorotryptophan-containing systems were no larger than variations noted between replicate simulations of the same systems. Interestingly, the B-factors for the fluorinated enzyme complex are better correlated with experiment (r_c = 0.62) than those obtained from simulations of the native (nonfluorinated) enzyme complex.

Fig. 4 *a* compares B-factors for backbone nitrogens of the native DHFR-methotrexate complex and those calculated from a 100-ps dynamics trajectory. The B-factors obtained from the simulation are similar to the crystallographic B-factors, r_c = 0.80, using enzyme B in the PDB file. A replicate simulation gave r_c = 0.62. In this case the crystal structure again was of high quality, with a resolution of 1.7 Å and a *R* value of 15.5% (Bolin et al., 1982). (It may be noted that the crystal contains two protein molecules per unit cell; the correlation coefficient for the B-factors of these is 0.78.) Introduction of 6-fluorotryptophan residues had little effect on the computed B-factors for the DHFR-MTX complex; simulations of this system gave calculated B-factors that also agreed with experiment (r_c = 0.49–0.53 in duplicate simulations).

Enzyme-MTX simulations using fully charged side chains showed more variability in their agreement between calculated and experimental B-factors (Fig. 5, *a* and *b*). In one simulation the calculated B-factors showed no correlation with experiment values (r_c of 0.04; Fig. 5 *a*). In this case, the greatest difference between experiment and simulation is in turn E (residues 63–73), where the calculated B-factors are no larger than average. The disagreement in this area is due to frequent dihedral transitions in the protein backbone. For this particular simulation, a dihedral transition does not take place in turn E until after 90 ps of production dynamics. A second simulation shows better agreement with experiment (r_c = 0.52; Fig. 5 *b*), exhibiting a correlation coefficient comparable to those obtained using B-factors obtained from simulations of systems with neutral residues.

Autocorrelation functions

The autocorrelation functions ($C_2(t)$) for all DHFR backbone N-H and C_α-H spin pairs were computed to examine

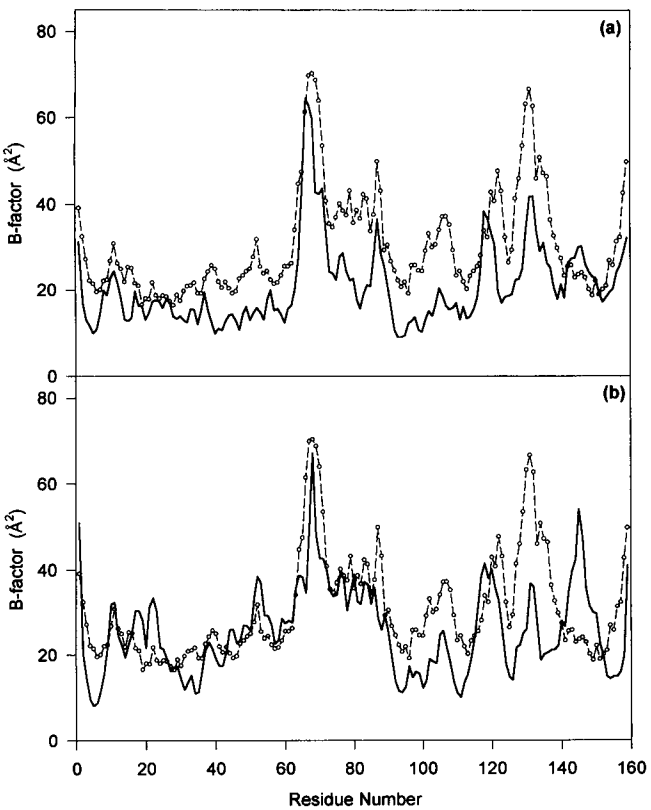

FIGURE 4 Comparison of calculated Debye-Waller B-factors (——) for backbone amide nitrogens with experiment (– – –). (*a*) Results from a simulation of the native DHFR-methotrexate complex. (*b*) Results from a simulation of the methotrexate-enzyme complex in which tryptophan residues of the protein have been replaced by 6-fluorotryptophan.

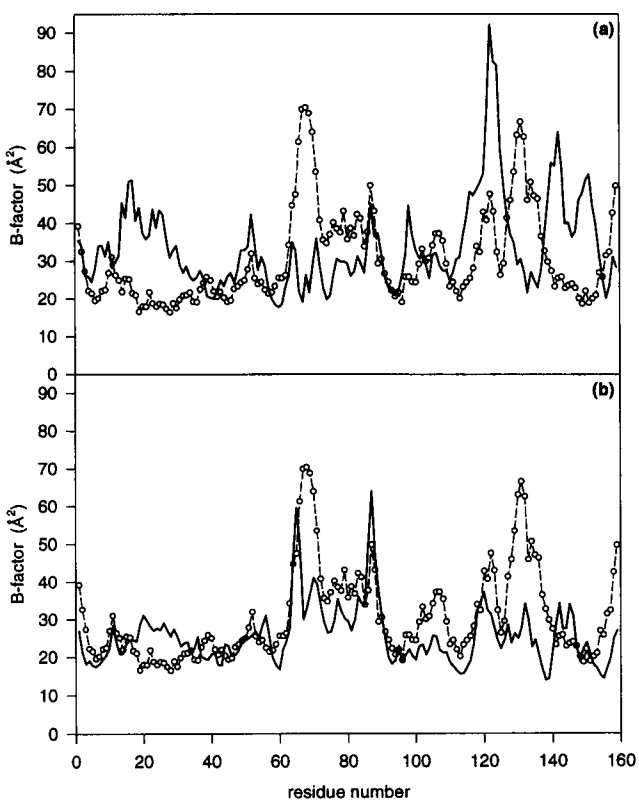

FIGURE 5 Comparison of calculated Debye-Waller B-factors (——) for backbone amide nitrogens with experiment (– – –). Both simulations are for fluorinated DHFR + MTX, using residues with full charges. The only difference between simulations is in the initial velocities.

the temporal aspects of the simulations. As has been observed in MD simulations by others, our calculated autocorrelation functions exhibited an initial burst phase in which there is a very rapid decay over a subpicosecond time period, followed by a slower decay. (For recent examples in other systems, see Palmer and Case (1992), Chandrasekhar et al. (1992), Smith et al. (1995), Yamasaki et al. (1995), and Philippopoulos and Lim (1995).) The burst phase observed for backbone N-H bonds was typically longer than the burst phase for the C_α-H systems, but in either case the correlation functions usually settled to a plateau value within tens of picoseconds. The early rapid phase seen in the calculated autocorrelation functions for backbone N-H and C_α-H bonds in the protein was also observed in the autocorrelation functions for bonds of the ligands, with the magnitude and time scale of the burst phase for the C-H and N-H bonds of the ligand similar to those of the backbone N-H and C_α-H bonds in secondary structures. Where feasible, the time constant (the effective internal correlation time, τ_e) characteristic of the decays of N-H and C_α-H bond correlation functions was estimated.

^{15}N NMR studies of mobility in the DHFR-folate complex have identified a range of time scales for internal motions in this system, as reflected in internal correlation times (τ_e) for N-H bond reorientation, that span a range from 3 to 6050 ps (Epstein et al., 1995). Table 1 compares correlation times calculated from our dynamics simulations of this complex to some of these experimental results.

TABLE 1 Comparison of Experimental and Calculated Correlation Times for DHFR + folate (all values are in picoseconds)

Residue	Experiment*	Native#	Fluorinated
Ala7	12 (16)	2	9
Glu17	20 (6)	32	
Trp22	10 (8)	19	15
Asn23	4 (6)	10, 1	
Arg33	6 (12)	12, 1	
Leu36	19 (10)	12, 3	17
Ile50	22 (7)	4	11
Gly51	8 (6)	4	
Gln65	12 (9)	24, 14	2
Ala83	14 (13)	5	2
Gly86	4 (7)	5, 6	
Met92	7 (16)	2	
Val93	3 (5)	10, 2	
Lys109	7 (15)	8	8
Tyr111	6 (11)	6	14
Ala117	10 (6)	25, 19	
Asp122	30 (7)	35	33
Glu129	12 (15)	11, 20	11
Asp131	40 (35)	15, 23	
Leu156	10 (8)	6	
Arg158	32 (13)	10	22

*Epstein et al., (1995); value in parenthesis indicates experimental range
#Correlation times for both native simulations. A single value indicates the other correlation time is below 1 ps.
Residues Thr46, Glu101, and Asp144 were omitted from this table because both native simulations of DHFR had correlation times below 1 ps.
A blank area corresponds to a correlation time below 1 ps.

Experimentally, there are 25 residues in the DHFR-folate complex that have τ_e for their N-H bonds that are less than 80 ps. These are the only residues that can feasibly be compared to the MD simulations. In duplicate simulations of the DHFR-folate complex, seven residues had calculated τ_e within the error range of the experimental τ_e in both, whereas 16 of the 25 residues had a calculated τ_e within the quoted error of the experimental value in at least one simulation. The correlation time for N-H bonds involved in secondary structures was usually below 15 ps, and many residues had values of τ_e of less than 5 ps. Correlation times for N-H bonds in residues found in turns and loops tended to be 20 ps or greater. No N-H bond vector of the complex had a τ_e greater than 40 ps in our MD simulations.

Fourteen correlation times (τ_e) calculated from the simulation of the 6-fluorotryptophan-containing DHFR-folate complex were within the error of the experimental values observed for the native DHFR-folate complex. This is the level of agreement of these correlation times with experiment exhibited by the native DHFR-folate complex, indicating that inclusion of fluorine in the protein does not significantly change any internal dynamics relative to the native system.

Similar correlation times for a given bond were not always obtained in replicate simulations. However, we emphasize that the calculation of τ_e from our data assumes only Woessner's simple model of reorientation about an axis (Woessner, 1962). The use of more elaborate models to characterize the differing decays of the autocorrelation function (Yamasaki et al., 1995) might produce better agreement between simulations in that they could be more responsive to details of the motions sampled during the simulation.

There are no published experimental τ_e values for the C_α-H bond vectors of DHFR from *Escherichia coli*. Correlation times (τ_e) for C_α-H bond calculated from our simulations are highly dependent on the location of the residue. If the residue is located in an area of secondary structure, the τ_e was usually below 5 ps. The τ_e for C_α-H bonds in flexible loops and turns ranged from 15 to 40 ps.

Backbone amide N-H bond order parameters and dihedral transitions

Order parameters (S^2) for backbone N-H bonds were calculated from the dynamics trajectories (Lipari and Szabo, 1982). A comparison of order parameters calculated from the averaged results of simulations to those found experimentally by analysis of ^{15}N NMR data for the native DHFR-folate complex (Table 2) shows that there is very good overall agreement of the calculations with experiment. Order parameters for backbone N-H bonds were also computed for the 6-fluorotryptophan-containing complexes of DHFR. There was very little difference between S^2 calculated for corresponding residues in the native or fluorine-containing complexes. As with other measures of structure

TABLE 2 Order Parameters for $N_{\epsilon 1}$-$H_{\epsilon 1}$ of Tryptophan Residues

	DHFR-folate (exp)	DHFR + folate (calc)	F-DHFR + folate (calc)	DHFR + MTX (calc)	F-DHFR + MTX (calc)
Trp22	0.91	0.83	0.91	0.84	0.91
Trp30	0.97	0.85	0.76	0.86	0.90
Trp47	0.85	0.86	0.89	0.78	0.90
Trp74	0.95	0.85	0.91	0.85	0.86
Trp133	0.90	0.84	0.92	0.85	0.89

and dynamics in these systems, the differences between order parameters calculated from simulations of 6-fluorotryptophan-containing complexes and complexes of the native enzyme were no larger than the variations observed from simulation to simulation in either the native or the fluorinated systems, and in any case agreed well with experimental results for the native (nonfluorinated) system. Although simulations of the fluorinated DHFR-MTX complex using charged side chains had a slightly larger range in mean S^2, there was no significant difference noted between simulations of enzyme-MTX complex with charged or neutral Asp, Glu, Lys, and Arg side chains.

Mean N-H bond order parameters (S^2) for structural regions of DHFR are tabulated in Table 2. The mean N-H bond S^2 was highest for the α-helices. For all simulations, and by experiment, the mean order parameters for β-sheets were less than those of the α-helices. Except for turn E, only minor differences were observed between order parameters calculated using the model with neutral side chains and the system in which Asp, Glu, Lys, and Arg side chains are charged. In turn E, the computed N-H bond S^2 was 0.76 in simulations using charged residues, whereas the mean of results from all simulations that used neutral residues was 0.60. The differences in order parameters for this region are due to the high S^2 calculated for Gly^{67} and Asp^{69} in both simulations done with charged residues; the dihedral transition that commonly occurs at Gly^{67} happened after 85 ps of production dynamics, which was too late to affect the calculation of S^2 according to our procedures.

Conformational flexibility appears to be an essential aspect of the catalytic activity of dihydrofolate reductase (Sawaya and Kraut, 1997). There are three regions within the structure of DHFR that show much conformational flexibility: loop 1, also known as the methionine loop (residues 9–23); turn E (residues 63–73); and the βF-βG loop region (residues 117–132). Presuming the same structure in solution as found in the crystalline state, all of these loops are solvent exposed. We observed in all simulations that backbone dihedral angle transitions within these regions are common, although it was not always the same residue in a region that underwent these conformational changes in a given simulation. Residues undergoing dihedral transitions within a certain region in different simulations were usually within one or two residues of each other; residues in these three regions typically had lower than average calculated N-H bond order parameters.

Each of these loops contains a glycine (Fig. 6). According to NMR results, Gly^{15} in loop 1 has a high S^2 of 0.88 and a short correlation time (0.08 ns). Gly^{121} has a lower S^2 of 0.50 and a longer τ_e of 0.6 ns, whereas Gly^{67} is most disordered ($S^2 = 0.29$), with a τ_e of $\sim$1.6 ns. In all of the simulations of DHFR, the computed order parameters for these glycines were consonant with these experimental results. The dihedral angle Φ formed by HN-N-CA-HA1 bond system was measured for these three glycines in all of the simulations. In simulations of the native enzyme-folate and MTX complexes, as well as the complexes formed with the 6-fluorotryptophan-substituted protein, the Φ angle of Gly^{15} shows a relatively restricted range during dynamics (Fig. 7). Over 100 ps there are high-frequency fluctuations of Φ for this residue within a single potential well, with deviations from average of about $\pm 15°$. Fig. 8 shows that the Φ angle for Gly^{121} in this system also tends to remain in a single potential well but, unlike Gly^{15}, the fluctuations in Φ are larger. Most of the conformation space of the potential well is sampled, which would result in a lower S^2 for this residue relative to Gly^{15}, as well as a longer correlation time. Infrequently a dihedral transition of this residue takes place (Fig. 8 *d*).

In all simulations of the DHFR complexes examined, the dynamics of Gly^{67} were vastly different from those of Gly^{15} and Gly^{121}. The Φ angle for Gly^{67} is prone to undergo dihedral transitions, even in the relatively short time frame of 100 ps (Fig. 9), and there is at least one dihedral transition during the trajectory of all of the simulations (except for fluorinated DHFR-folate complex), and two or three dihedral transitions are often observed. Frequent dihedral transitions would appear to account for the extremely low experimental S^2 and long τ_e of 1.6 ns found experimentally for this residue.

The dynamical behavior exhibited by these three glycines in the simulations using neutral residues was also apparent in simulations using residues with full charges. Fig. 10 shows the variations of Φ for residues Gly^{121} and Gly^{67} for two charged simulations during production dynamics. A single dihedral transition occurs in Gly^{121} in one of the simulations. Gly^{67} undergoes a dihedral transition in both simulations after 85 ps. The dynamics of Gly^{15} are similar to those observed in simulations with neutral residues.

Loop 1 of DHFR (residues 9–23) has been implicated in controlling the rate of catalysis for this enzyme (Farnum et al., 1991; Li et al., 1992; Sawaya and Kraut, 1997). In

contrast to crystal structures of other forms of DHFR, in DHFR-MTX and DHFR-folate complexes loop 1 is ordered and coordinates have been assigned for all of the heavy backbone atoms that comprise the loop. All of our simulations of DHFR show that this region tends to be flexible, regardless of the nature of the bound ligand.

Turn E and the βF-βG loop are also important for both the stability of the protein and catalysis. Single point mutations of the glycines at position 67 or 121 adversely affect the stability of the enzyme and the rate of hydride transfer, presumably because the mutations alter the conformation and flexibility of the loops (Gekko et al., 1994; Ohmae et al., 1996). However, it is currently unclear how either of these two loops could influence catalysis directly, because Gly^{121} is 19 Å and Gly^{67} is almost 30 Å away from the critical Asp^{27} residue at the active site.

The residues in turn E, especially residues 67–69, consistently had the lowest calculated order parameters. ^{15}N NMR data confirm that turn E is the most flexible region of the protein in the DHFR-folate complex. Although the NMR data indicate that the βF-βG loop region is not significantly more mobile than other regions of the protein, calculated order parameters from simulations of the DHFR-folate and DHFR-MTX complexes indicate that the N-H bonds of many residues in this part of the structure undergo large-scale reorientations. B-factors from DHFR crystal structures are consistent with the conclusion that this segment of the protein undergoes large spatial fluctuations; residues with the highest B-factors are consistently located in this part of the structure.

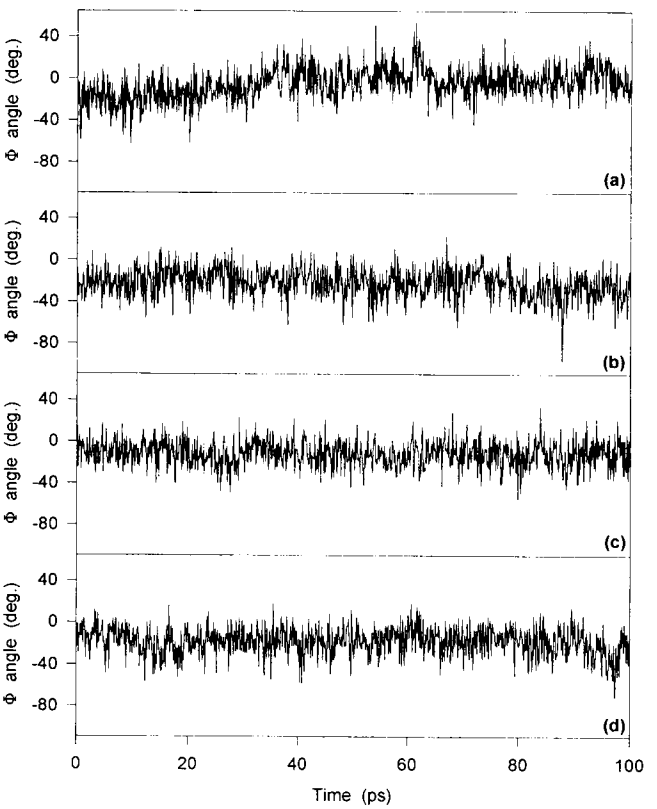

FIGURE 7 Changes of the dihedral angle Φ of glycine-15 during the course of a 100-ps dynamics simulation of (*a*) the native DHFR-folate complex, (*b*) the 6-fluorotryptophan-containing DHFR-folate complex, (*c*) the native DHFR-MTX complex, and (*d*) the 6-fluorotryptophan-containing DHFR-MTX complex.

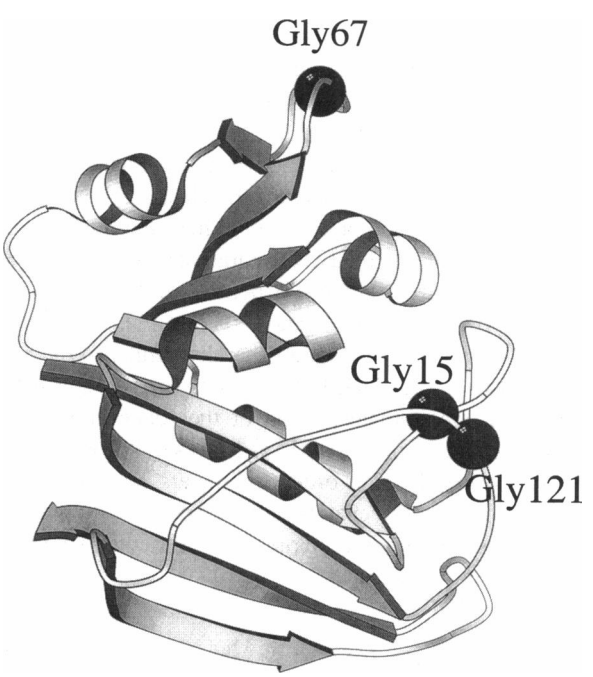

FIGURE 6 A schematic rendering of DHFR (*E. coli*). Glycines in the flexible loops discussed in the text are represented by the spheres. The drawing was generated by MOLSCRIPT (Kraulis, 1991).

There appears to be an intriguing correlation between the average order parameter (S^2) for the N-H bonds of turn E (residues 67–69) and those for residues 120–122, a portion of the βF-βG loop. The correlation is found only in simulations of the folate and MTX complexes and not in simulations of other DHFR systems (E. Lau, work in progress); the correlation is also reflected in order parameters for C_α-H bond in these residues. For residues 67–69 the mean N-H bond S^2 in the folate and MTX binary complexes was below 0.70, whereas in simulations of other complexes or the apoenzyme, S^2 was greater than 0.70. The experimental values for residues 67 and 69 were 0.29 and 0.58, respectively. (An experimental value for residue 68 was not determined.) Similarly, calculated order parameters for N-H bonds in residues 120–122 in simulations of the folate and MTX complexes are consistently less than 0.75, whereas these parameters for simulations of other forms of the enzyme are greater than 0.75. (Experimental values for residues 120–122 are 0.72, 0.50, and 0.68, respectively.) Thus increased disorder of residues of turn E and the βF-βG loop in the binary complexes appears simultaneously, although this is not observed in simulations of other complexes or the apoenzyme. It is not apparent how the motions

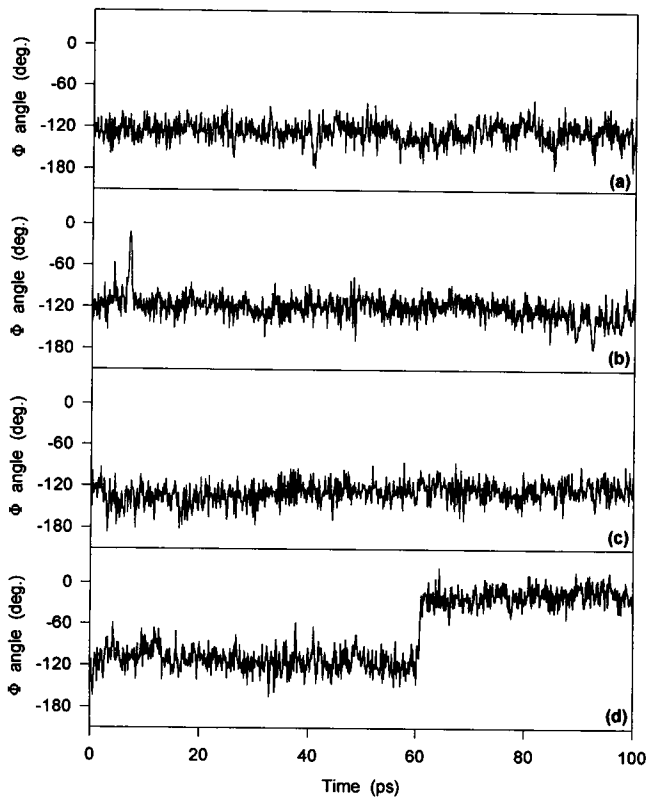

FIGURE 8 Changes of the dihedral angle Φ of glycine-121 during the course of a 100-ps dynamics simulation of (*a*) the native DHFR-folate complex, (*b*) the 6-fluorotryptophan-containing DHFR-folate complex, (*c*) the native DHFR-MTX complex, and (*d*) the 6-fluorotryptophan-containing DHFR-MTX complex.

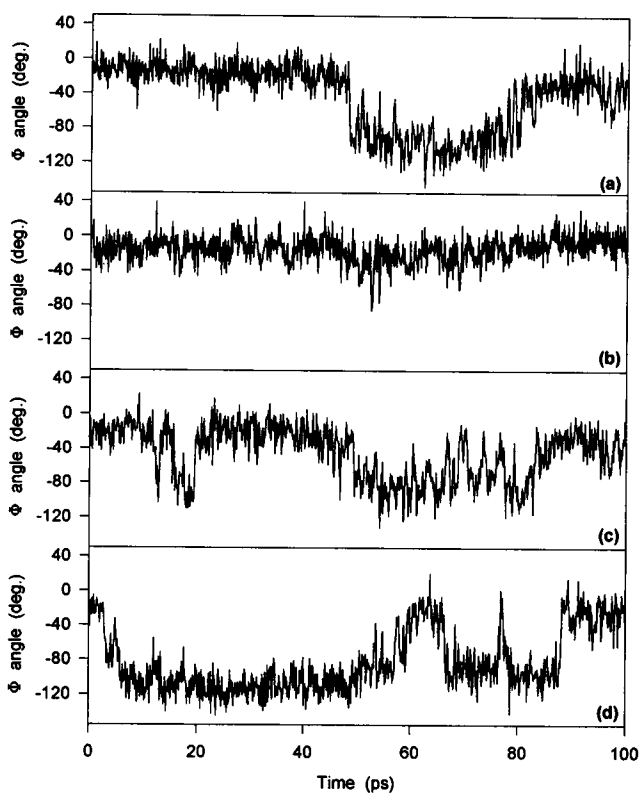

FIGURE 9 Changes of the dihedral angle Φ of Gly^{67} during the course of a 100-ps dynamics simulation of (*a*) the native DHFR-folate complex, (*b*) the 6-fluorotryptophan-containing DHFR-folate complex, (*c*) the native DHFR-MTX complex, and (*d*) the 6-fluorotryptophan-containing DHFR-MTX complex.

of these two loops become codependent; a direct correlation of their motions seems unlikely because these residues are separated by over 27 Å.

Order parameters for C_α-H bonds

Order parameters for backbone C_α-H bonds calculated from our simulation were usually higher than the backbone N-H bond S^2 values in corresponding amino acids (Fig. 11). This observation has been routinely made in other MD simulations (for examples see Palmer and Case, 1992; Smith et al., 1995; Philippopoulos and Lim, 1995), and a summary of possible reasons has been offered by Philippopoulos and Lim (1995). In our work the range of average order parameters calculated for the backbone N-H bonds was 0.75–0.78; the range for the average S^2 values for the C_α-H calculated from the same MD trajectories was 0.85–0.87. In the simulations there was always at least one residue in turn E that had a C_α-H order parameter below 0.50. Interestingly, only simulations of these binary complexes unusually exhibit mobility in this loop; it is not detected in simulations of the apoenzyme or other complexes (E. Lau, work in progress).

Ligand order parameters

Order parameters were calculated for all C-H and N-H bonds of the ligands in the DHFR complexes. The average of calculated S^2 values for MTX in the DHFR-MTX complex ranged from 0.85 to 0.90, including order parameters for the amino groups of MTX, and was independent of whether the model used neutral or charged side chains. All NH groups of MTX form hydrogen bonds with either the protein or with water molecules. Computed order parameters for all spin pairs of the *p*-aminobenzoylglutamate portion of MTX were also high. Order parameters for ligand N-H and C-H spin pairs of the DHFR-folate complex were generally similar to the corresponding parts of the DHFR-MTX complex, except that the *p*-aminobenzoylglutamate portion of the folate complex appears to be more mobile, with S^2 as low as 0.49 for some spin pairs. The generally high order parameters for spin pairs of MTX and folate in the enzyme complexes indicate that these two ligands do not undergo large-scale reorientations relative to their protein partner.

Order parameters for the $N_{\epsilon 1}$-$H_{\epsilon 1}$ bond of 6-fluorotryptophan and tryptophan

Order parameters calculated for the $N_{\epsilon 1}$-$H_{\epsilon 1}$ bond of the 6-fluorotryptophan and tryptophan residues calculated from

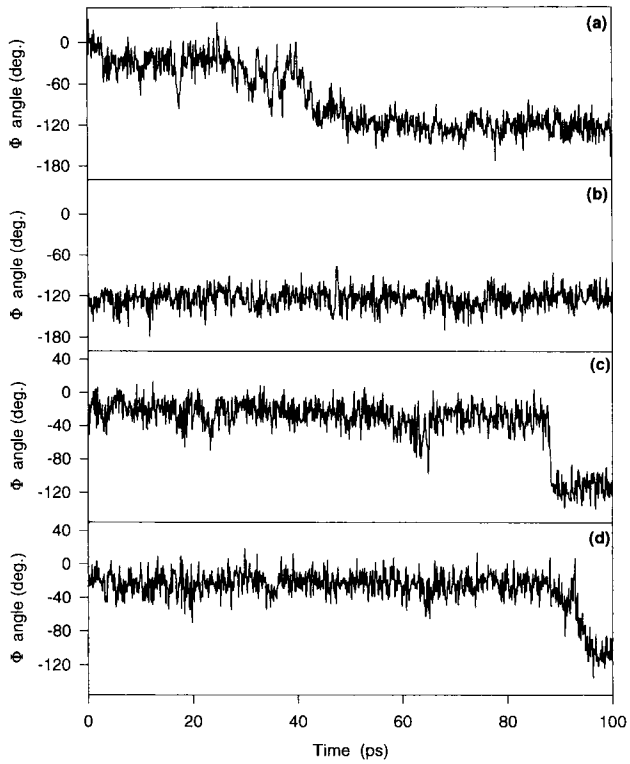

FIGURE 10 Changes in the dihedral angle Φ of Gly^{121} and Gly^{67} during the course of a 100-ps dynamics simulation using residues with full charges. The dihedral angle Φ of Gly^{121} from the two simulations is shown in *a* and *b*, and Φ for Gly^{67} is shown in *c* and *d*.

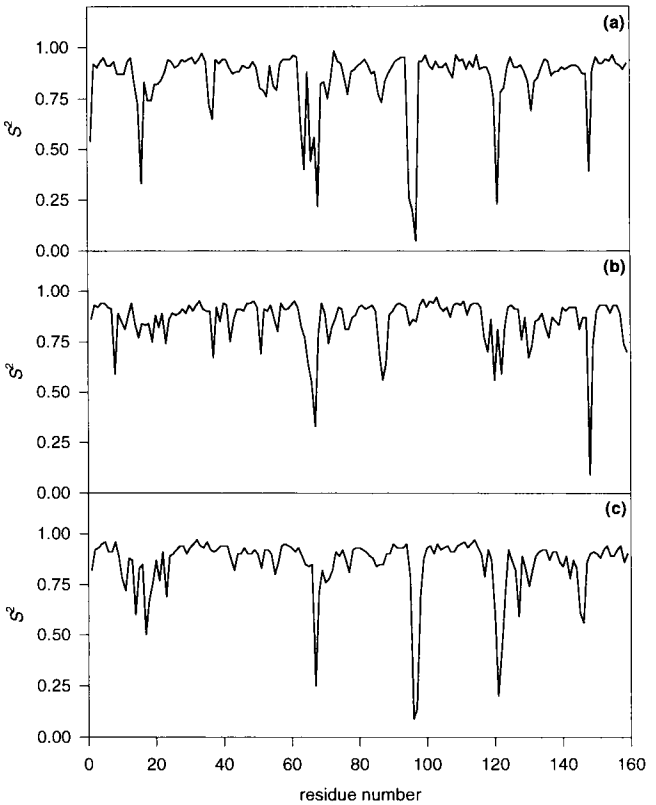

FIGURE 11 Calculated C_α-H order parameters S^2 from a molecular dynamics simulation of the native DHFR-folate complex (*a*), native DHFR-MTX complex (*b*), and fluoro-DHFR-MTX using fully charged residues (*c*).

simulations of their respective folate and MTX complexes were somewhat smaller than the order parameters found experimentally for these groups in the native DHFR-folate complex by ^{15}N NMR studies (Table 3). The addition of fluorine to the indole ring does not seem to affect the dynamics of the ring, because there was no discernible difference between the calculated N-H S^2 values at corresponding positions for the 6-fluorotryptophan and tryptophan forms of the complexes. Although the failure of the simulations to reproduce the behavior of the $N_{\epsilon 1}$-$H_{\epsilon 1}$ bonds better is not understood, the near-identity of computed indole N-H order parameters for native and the 6-fluorotryptophan-complexes of DHFR argues that the fluorine substitution has little effect on indole ring dynamics. The S^2 for the $N_{\epsilon 1}$-$H_{\epsilon 1}$ bond vector for the fluorotryptophans from simulations using fully charged residues are similar to those obtained with neutral residues.

There is an experimental value for the correlation time τ_e for only one $N_{\epsilon 1}$-$H_{\epsilon 1}$ bond vector: Trp^{133} has a τ_e of 35 ± 23 ps (Epstein et al., 1995). The calculated τ_e for this bond vector was found to be 11 and 22 ps in the two DHFR-folate simulations, both in reasonable accord with experiment.

Folate and NADPH binding sites

^{15}N NMR studies have shown that residues comprising the NADPH-binding site of DHFR-folate complex (residues 5, 6, 7, 44, 46, 63, 76, 77, 78, 94, 95, 96, 99, 100, 102, 123) are as restricted toward angular reorientation as residues in the occupied folate site (residues 5, 6, 7, 20, 22, 27, 28, 30, 31, 32, 50, 54, 94). The average experimental S^2 for backbone N-H of the residues comprising these two regions are 0.83 and 0.80, respectively. Thus the order parameters for these two regions are approximately the same as the average order parameter (0.81) characteristic of the entire protein. Simulations of the DHFR-folate complex reproduce the conformational restriction of both binding sites, with the mean S^2 for the occupied folate site being 0.85 in replicate simulations. The average N-H bond order parameter calculated for the empty NADPH-binding site was 0.79–0.82 in these simulations. The addition of fluorine to the DHFR + folate complex did not affect the conformational restriction of either the folate or NADPH binding sites.

Similar results are obtained from simulations of the DHFR-MTX complex, and the average S^2 for either binding site was not affected by the inclusion of the 6-fluorotryptophans or the charges of the residues. The mean N-H bond S^2 for residues defining the (occupied) folate site was 0.82–0.85 in simulations of the native DHFR-folate complex and 0.79–0.83 in simulations of the corresponding fluorinated system. The average order parameter for N-H bonds in the unoccupied NADPH binding site ranged from 0.83–0.85 for

the nonfluorinated case and 0.81–0.82 for the 6-fluorotryptophan-containing DHFR-MTX complex. The average S^2 for the occupied folate site was 0.85–0.86 for simulations with charged residues, and the empty NADPH site had average S^2 values of 0.82–0.83.

A conformational change within the protein accompanies binding of methotrexate to apo-DHFR. This includes a ~6° relative rotation of the adenine binding domain and a shift of helix B by ~0.5 Å (Bystroff and Kraut, 1991). A similar but smaller conformational change is found when folate is bound to apo-DHFR (Reyes et al., 1995). From our simulations, we find that these conformational changes do not significantly change the N-H bond order parameters for either binding site, and it appears that the folate-binding site is just as rigid when occupied as when unoccupied (E. Lau, work in progress).

DISCUSSION

There have been crystallographic studies of fluorine-containing proteins or protein-ligand complexes. However, in most cases the fluorine is part of the ligand, such as trifluoromethyl ketone, and is chemically situated so that it has a direct chemical effect on the interaction/reaction of the ligand with the protein. By their nature, these structures usually do not provide much information regarding the effects of simply changing a C-H bond to a C-F bond in a nonreactive part of the structure. Crystallographic studies of small proteins containing fluorinated aromatic residues or NMR structural studies of ^{15}N-labeled analogs of such proteins, while highly desirable in this context, have not appeared. Until studies of such multiply labeled systems are available, theoretical simulations provide a bridge between experimental studies of native (but ^{15}N-labeled) dihydrofolate reductase and an analog of the protein in which all tryptophan residues have been replaced by 6-fluorotryptophan.

Many aspects of our simulations of the DHFR-folate complex are in good agreement with experimental results, including the Debye-Waller (B) factors as defined by crystallographic efforts (solid state), and backbone N-H bond order parameters in solution. The simulations reflect the conformational rigidity of the occupied folate-binding site and the empty NADPH-binding site seen in the nitrogen NMR results. Thus, although the time period of the simulations is short, our computational models appear to accurately capture features of the structures and dynamics of the folate and methotrexate complexes of DHFR.

The ability of the ligands MTX and folate to alter the dynamics of a flexible loop over 10 Å away from any atom of the ligand, and the apparent correlation between motions in turn E and the βF-βG loop, despite their appreciable separation, are features of the simulations that are potentially significant for understanding the stability and mechanism of action of DHFR. An elucidation of these facets of our simulations would appear to require the availability of longer dynamics trajectories and investigation of the dependence of these observations on the parameters of the model.

Accepting that our structural models and simulations provide reasonably reliable indications of structure and dynamics in solvated dihydrofolate reductase, it is clear that introduction of 6-fluorotryptophan into DHFR does not significantly alter the structure or perturb the dynamics of the enzyme in DHFR-folate or DHFR-methotrexate complexes, at least on the time scale sampled by these MD simulations. The C-F for C-H change at a tryptophan residue leads to many small adjustments of the positions of atoms surrounding the fluorotryptophan side chains to accommodate the halogen. These changes apparently are so small that they are not reliably reflected in statistics such as the RMS deviations. It thus may require a very strongly diffracting crystal before an x-ray structural study would show significant differences between the fluorinated and native system.

Mobilities of the backbone and side chains of the fluoroenzyme are computed to be virtually identical to their counterparts in the native enzyme. It has been observed that DHFR in which the 6-fluoroanalog replaces tryptophan residues has "enzyme activity and stability nearly identical to those of the unlabeled wild-type protein," although details are not given (Hoeltzli and Frieden, 1994). The results of our calculations are consistent with this report.

We thank Prof. M. Karplus (Harvard University) for supplying copies of the CHARMM program.

This work was supported in part by the U.S. Public Health Service through National Institutes of Health grant GM 25975 and the University of California–Santa Barbara Committee on Research.

REFERENCES

Blakley, R. L. 1995. Eukaryotic dihydrofolate reductase. *Adv. Enzymol.* 70:23–102.

Bolin, J. T., D. J. Filman, D. A. Matthews, R. C. Hamlin, and J. Kraut. 1982. Crystal structures of *Escherichia coli* and *Lactobacillus casei* dihydrofolate reductase refined at 1.7 Å resolution. I. General features and binding of methotrexate. *J. Biol. Chem.* 257:13650–13662.

Brooks, B. R., R. E. Bruccoleri, B. D. Olafson, D. J. States, S. Swaminathan, and M. Karplus. 1983. CHARMM: a program for macromolecular energy minimization and dynamics calculations. *J. Comput. Chem.* 4:187–217.

Bystroff, C., and J. Kraut. 1991. Crystal structure of unliganded *Escherichia coli* dihydrofolate reductase. Ligand-induced conformational changes and cooperativity in binding. *Biochemistry.* 30:2227–2239.

Bystroff, C., S. J. Oatley, and J. Kraut. 1990. Crystal structures of *Escherichia coli* dihydrofolate reductase: the $NADP^+$ holoenzyme and the folate·$NADP^+$ ternary complex. Substrate binding and a model for the transition state. *Biochemistry.* 29:3263–3277.

Chandrasekhar, I., G. M. Clore, A. Szabo, A. M. Gronenborn, and B. R. Brooks. 1992. A 500 ps molecular dynamics simulation study of interleukin-1β in water. *J. Mol. Biol.* 226:239–250.

Cummins, P. L., K. Ramnarayan, U. C. Singh, and J. E. Gready. 1991. Molecular dynamics/free energy perturbation study on the relative affinities of the binding of reduced and oxidized NADP to dihydrofolate reductase. *J. Am. Chem. Soc.* 113:8247–8256.

Danielson, M. A., and J. J. Falke. 1996. Use of ^{19}F NMR to probe protein structure and conformational changes. *Annu. Rev. Biophys. Biomol. Struct.* 25:163–195.

Epstein, D. M., S. J. Benkovic, and P. E. Wright. 1995. Dynamics of the dihydrofolate reductase-folate complex: catalytic sites and regions

known to undergo conformational change exhibit diverse dynamical features. *Biochemistry.* 34:11037–11048.

Farnum, M. F., D. Magde, E. E. Howell, J. T. Hirai, M. S. Warren, J. K. Grimsley, and J. Kraut. 1991. Analysis of hydride transfer and cofactor fluorescence decay in mutants of dihydrofolate reductase: possible evidence for participation of enzyme molecular motions in catalysis. *Biochemistry.* 30:11567–11579.

Fierke, C. A., K. A. Johnson, and S. J. Benkovic. 1987. Construction and evaluation of the kinetic scheme associated with dihydrofolate reductase from *Escherichia coli. Biochemistry.* 26:4085–4094.

Gasteiger, J., and M. Marsili. 1980. Iterative partial equalization of orbital electronegativity—a rapid access to atomic charges. *Tetrahedron.* 36: 3219–3228.

Gavezzotti, A. 1983. The calculation of molar volumes and the use of volume analysis in the investigation of structured media and of solid state organic reactivity. *J. Am. Chem. Soc.* 105:5220–5225.

Gekko, K., Y. Kunori, H. Takeuchi, S. Ichihara, and M. Kodama. 1994. Point mutations at glycine-121 of *Escherichia coli* dihydrofolate reductase: important roles of a flexible loop in the stability and function. *J. Biochem.* 116:34–41.

Gerig, J. T. 1994. Fluorine NMR of proteins. *Prog. NMR Spectrosc.* 26:293–370.

Gerothanassis, I. P., B. Birdsall, C. J. Bauer, T. A. Frenkiel, and J. Feeney. 1992. NMR detection of bound water molecules in the active site of *L. casei* dihydrofolate reductase in aqueous solution. *J. Mol. Biol.* 226: 549–554.

Gregory, D. H., and J. T. Gerig. 1989. Force field parameterization for the 4-fluorophenyl group. *J. Comput. Chem.* 10:711–717.

Gregory, D. H., and J. T. Gerig. 1991. Prediction of fluorine chemical shifts in proteins. *Biopolymers.* 31:845–858.

Hoeltzli, S. D., and C. Frieden. 1994. ^{19}F NMR spectroscopy of [6-F]tryptophan-labeled *Escherichia coli* dihydrofolate reductase: equilibrium folding and ligand binding studies. *Biochemistry.* 33:5502–5509.

Hortin, G., and I. Boime. 1983. Applications of amino acid analogs for studying co- and posttranslational modifications of proteins. *Methods Enzymol.* 96:777–784.

Ichiye, T., B. D. Olafson, S. Swaminathan, and M. Karplus. 1986. Structure and internal mobility of proteins: a molecular dynamics study of hen egg white lysozyme. *Biopolymers.* 25:1909–1937.

Jorgensen, W. L., J. Chandrasekhar, J. D. Madura, R. W. Impley, and M. L. Klein. 1983. Comparison of simple potential functions for simulating liquid water. *J. Chem. Phys.* 79:926–935.

Kraulis, P. 1991. MOLSCRIPT: a program to produce both detailed and schematic plots of protein structures. *J. Appl. Crystallogr.* 24:946–950.

Lau, E. Y., and J. T. Gerig. 1996. Solvent effects on the fluorine shielding of fluorobenzene. *J. Am. Chem. Soc.* 118:1194–1200.

Leo, A., C. Hantsch, and D. Elkins. 1971. Partition coefficients and their uses. *Chem. Rev.* 71:525–616.

Li, L., C. J. Falzone, P. E. Wright, and S. J. Benkovic. 1992. Functional role of a mobile loop of *Escherichia coli* dihydrofolate reductase in transition-state stabilization. *Biochemistry.* 31:7826–7833.

Lipari, G., and A. Szabo. 1982. Model-free approach to the interpretation of nuclear magnetic resonance relaxation in macromolecules. 1. Theory and range of validity. *J. Am. Chem. Soc.* 104:4546–4559.

McCammon, J. A., and S. C. Harvey. 1987. Dynamics of Proteins and Nucleic Acids. Cambridge University Press, Cambridge.

McDonald, J. J., and C. L. Brooks. 1992. A theoretical approach to drug design. 3. Relative thermodynamics of inhibitor binding by *E. coli* dihydrofolate reductase to ethyl derivatives of trimethoprim substituted at the 3′-position, 4′-position, and 5′-position. *J. Am. Chem. Soc.* 114: 2062–2072.

Meiering, E. M., H. Li, T. J. Delcamp, J. H. Freisheim, and G. Wagner. 1995. Contributions of tryptophan 24 and glutamate 30 to binding long-lived water molecules in the ternary complex of human dihydrofolate reductase with methotrexate and NADPH studied by site-directed mutagenesis and nuclear magnetic resonance spectroscopy. *J. Mol. Biol.* 247:309–325.

Meiering, E. M., and G. Wagner. 1995. Detection of long-lived bound water molecules in complexes of human dihydrofolate reductase with methotrexate and NADPH. *J. Mol. Biol.* 247:294–308.

Momany, F. A., and R. Rone. 1992. Validation of the general purpose QUANTA 3.2/CHARMm force field. *J. Comput. Chem.* 13:888–900.

Noren, G. J., S. J. Anthony-Cahill, M. C. Griffiths, and P. G. Shultz. 1989. A general method for site-specific incorporation of unnatural amino acids into proteins. *Science.* 244:182–188.

Nyberg, S. C., and C. H. Faerman. 1985. A revision of van der Waals atomic radii for molecular crystals: N, O, F, Se, Br, and I bonded to carbon. *Acta Crystallogr.* B41:264–278.

Oefner, C., A. D'Arcy, and F. K. Winkler. 1988. Crystal structure of human dihydrofolate reductase complexed with folate. *Eur. J. Biochem.* 174:377–384.

Ohmae, E., K. Iriyama, S. Ichihara, and K. Gekko. 1996. Effects of point mutations at the flexible loop glycine-67 of *Escherichia coli* dihydrofolate reductase on its stability and function. *J. Biochem.* 119:703–710.

Palmer, A. G., and D. A. Case. 1992. Molecular dynamics analysis of NMR relaxation in a zinc-finger peptide. *J. Am. Chem. Soc.* 114: 9059–9067.

Pearson, J. G., E. Oldfield, F. S. Lee, and A. Warshel. 1993. Chemical shifts in proteins: a shielding trajectory analysis of the fluorine nuclear magnetic resonance spectrum of the *Escherichia coli* galactose binding protein using a multipole shielding polarizability-local reaction field-molecular dynamics approach. *J. Am. Chem. Soc.* 115:6851–6862.

Penner, M. H., and C. Frieden. 1987. Kinetic analysis of the mechanism of *Escherichia coli* dihydrofolate reductase. *J. Biol. Chem.* 262: 15908–15914.

Petsko, G. A., and D. Ringe. 1984. Fluctuations in protein structure from X-ray diffraction. *Annu. Rev. Biophys. Bioeng.* 13:331–371.

Philippopoulos, M., and C. Lim. 1995. Molecular dynamics simulation of *E. coli* ribonuclease H_1 in solution: correlation with NMR and X-ray data and insights into biological function. *J. Mol. Biol.* 254:771–792.

Polygen. 1990. QUANTA 3.0 Parameter Handbook. Polygen, Waltham, MA.

Reyes, V. M., M. R. Sawaya, K. A. Brown, and J. Kraut. 1995. Isomorphous crystal structures of *Escherichia coli* dihydrofolate reductase complexed with folate, 5-deazafolate, and 5,10-dideazatetrahydrofolate: mechanistic implications. *Biochemistry.* 34:2710–2723.

Ryckaert, J. P., G. Ciccotti, and H. J. C. Berendsen. 1977. Numerical integration of the Cartesian equations of motion of a system with constraints: molecular dynamics of *n*-alkanes. *J. Comput. Phys.* 23: 327–341.

Sawaya, M. R., and J. Kraut. 1997. Loop and subdomain movements in the mechanism of *Escherichia coli* dihydrofolate reductase: crystallographic evidence. *Biochemistry.* 36:586–603.

Searle, M. S., M. J. Forster, B. Birdsall, G. K. C. Roberts, J. Feeney, H. T. A. Cheung, I. Kompis, and A. J. Geddes. 1988. Dynamics of trimethoprim bound to dihydrofolate reductase. *Proc. Natl. Acad. Sci. USA.* 85:3787–3791.

Singh, U. C. 1988. Probing the salt bridge in the dihydrofolate reductase-methotrexate complex by using the coordinate-coupled free-energy perturbation method. *Proc. Natl. Acad. Sci. USA.* 85:4280–4282.

Singh, U. C., and S. J. Benkovic. 1988. A free energy perturbation study of the binding of methotrexate to mutants of dihydrofolate reductase. *Proc. Natl. Acad. Sci. USA.* 85:9519–9523.

Smith, L. J., and C. M. Dobson. 1996. NMR and protein dynamics. *Int. J. Quant. Chem.* 59:315–332.

Smith, P. E., R. C. van Schaik, T. Szyperski, K. Wuthrich, and van W. R. Gunsteren. 1995. Internal mobility of the basic pancreatic trypsin inhibitor in solution: a comparison of NMR spin relaxation measurements and molecular dynamics simulations. *J. Mol. Biol.* 246:356–365.

Smyth, C. P., and K. B. McAlpine. 1934. The dipole moment of the methyl and ethyl halides. *J. Chem. Phys.* 2:499–502.

Tasaki, K., S. McDonald, and J. W. Brady. 1993. Observations concerning the treatment of long-range interactions in molecular dynamics simulations. *J. Comput. Chem.* 15:667–683.

Verlet, L. 1967. Computer experiments on classical fluids. I. *Phys. Rev.* 159:98–113.

Verma, C. S., L. S. D. Caves, R. E. Hubbard, and G. C. K. Roberts. 1997. Domain motions in dihydrofolate reductase: a molecular dynamics study. *J. Mol. Biol.* 266:776–796.

Wagner, G., S. Hyberts, and J. W. Peng. 1993. Study of Protein Dynamics for NMR, in NMR of Proteins. G. M. Clore and A. M. Gronenborn, editors. CRC Press, Boca Raton, FL. 220–257.

Wallace, C. J. A. 1978. Semisynthetic analogues of cytochrome c: modifications to fragment (66–104). *In* Semisynthetic Peptides and Proteins. R. E. Offord and C. Di Bello, editors. Academic, New York. 101–114.

Woessner, D. E. 1962. Spin relaxation processes in a two-proton system undergoing anisotropic reorientation. *J. Chem. Phys.* 36:1–4.

Yamasaki, K., M. Saito, M. Oobatake, and S. Kanaya. 1995. Characterization of the internal motions of *Escherichia coli* ribonuclease HI by a combination of ^{15}N-NMR relaxation analysis and molecular dynamics simulation: examination of dynamics model. *Biochemistry.* 34: 6587–6601.